

Drug Discovery

How to cite: *Angew. Chem. Int. Ed.* **2021**, *60*, 10547–10551

International Edition: doi.org/10.1002/anie.202015422

German Edition: doi.org/10.1002/ange.202015422

Selective Inhibition of the Hsp90 α Isoform

Sanket J. Mishra, Anuj Khandelwal, Monimoy Banerjee, Maurie Balch, Shuxia Peng, Rachel E. Davis, Taylor Merfeld, Vitumbiko Munthali, Junpeng Deng, Robert L. Matts, and Brian S. J. Blagg*

Abstract: The 90 kDa heat shock protein (Hsp90) is a molecular chaperone that processes nascent polypeptides into their biologically active conformations. Many of these proteins contribute to the progression of cancer, and consequently, inhibition of the Hsp90 protein folding machinery represents an innovative approach toward cancer chemotherapy. However, clinical trials with Hsp90 N-terminal inhibitors have encountered deleterious side effects and toxicities, which appear to result from the pan-inhibition of all four Hsp90 isoforms. Therefore, the development of isoform-selective Hsp90 inhibitors is sought to delineate the pathological role played by each isoform. Herein, we describe a structure-based approach that was used to design the first Hsp90 α -selective inhibitors, which exhibit >50-fold selectivity versus other Hsp90 isoforms.

Molecular chaperones are a class of proteins that regulate proteostasis by assisting in the conformational maturation of nascent polypeptides (referred to as client proteins) and the renaturation of denatured proteins. The heat shock proteins (Hsps) belong to a ubiquitously expressed molecular chaperone family that is highly conserved in eukaryotes. In fact, the 90 kDa Heat shock protein (Hsp90) is one of the most abundant Hsps and is highly upregulated in stressed cells, including cancer.^[1,2] As a molecular chaperone, Hsp90 is responsible for the conformational maturation of more than 300 client protein substrates, many of which are key regulators of oncogenic transformation, growth, and metastasis.^[3–6] As a result, Hsp90 has been widely sought after as a cancer target, which resulted in the development of 18 inhibitors that underwent clinical evaluation.^[7,8] Unfortunately, the clinical approval of these inhibitors was hindered due to detrimental activities that are likely to result from the inhibition of all four Hsp90 isoforms (*pan*-inhibitors). The four Hsp90 isoforms include cytosolic isoforms Hsp90 α (inducible) and Hsp90 β (constitutively expressed); the endo-

plasmic reticulum residing glucose regulated protein 94 (Grp94); and the mitochondrial isoform, tumor necrosis factor receptor-associated protein 1 (Trap1).^[1,2] *Pan*-inhibition of all four isoforms leads to non-specific degradation of the entire Hsp90-dependent substrate population, and ultimately leads to undesired activities.^[4,9] The development of Hsp90 isoform-selective compounds can provide a tool to dissect the role played by each isoform towards disease pathology and toxicities associated with pan Hsp90 inhibition.

Despite high structural similarity between the constitutively expressed isoform, Hsp90 β , and the inducible isoform, Hsp90 α , each of these isoforms fold select client proteins.^[10] Genetic knockdown of Hsp90 α results in the degradation of oncogenic client proteins, suggesting that the administration of an Hsp90 α -selective inhibitor could exhibit anti-cancer activity against Hsp90 α -dependent cancers.^[11] In addition to its presence in the cytosol, Hsp90 α is also secreted extracellularly to promote wound healing, cell adhesion, and inflammation.^[12] In fact, significant levels of Hsp90 α are secreted from highly invasive cancers to activate matrix metalloproteinase 2 (MMP-2) to induce expression of MMP-3, which drives tumor invasion.^[13,14]

Extracellular Hsp90 α also contributes to an inflammatory microenvironment that supports prostate cancer progression.^[14] Analysis of gene ontology traits revealed Hsp90 β to interact with a larger subset of proteins than Hsp90 α .^[15] Notably, Hsp90 α -dependent processes contribute to stress adaptation or other specialized functions, while Hsp90 β is important for maintaining cell viability, clearly highlighting the distinct evolution of each isoform.^[15–17]

Initial efforts to develop isoform-selective inhibitors focused on Grp94, due to its distinguishing structural features that easily differentiate it from the other Hsp90 isoforms.^[18–20] However, the design of isoform-selective inhibitors against the cytosolic isoforms, Hsp90 α and Hsp90 β , has been extremely challenging as these isoforms share > 95% identity within the N-terminal ATP-binding sites. In fact, only two amino acids differ between these nucleotide-binding sites. Despite these challenges, we recently disclosed **KUNB 31** as the first Hsp90 β -selective inhibitor.^[21] However, an isoform selective inhibitor of Hsp90 α has not yet been reported. Upon analysis of the Hsp90 α and β N-terminal ATP-binding sites bound to radicicol (Figure 1), it was determined that the resorcinol moiety interacts uniquely with each Hsp90 isoform. Compound **1** was chosen as lead molecule because it represents an analog of AT13387, which is a resorcinol-derived Hsp90 *pan*-inhibitor that underwent clinical evaluation.^[2] Computational studies with **1** bound to the N-terminal ATP-binding site of Hsp90 α (PDB: 2XAB) and Hsp90 β

[*] Dr. S. J. Mishra, A. Khandelwal, Dr. M. Banerjee, R. E. Davis, T. Merfeld, V. Munthali, Prof. Dr. B. S. J. Blagg
Department of Chemistry and Biochemistry
The University of Notre Dame
305 McCourtney Hall, Notre Dame, IN 46556 (USA)
E-mail: bblagg@nd.edu

Dr. M. Balch, Dr. S. Peng, Dr. J. Deng, Prof. Dr. R. L. Matts
Department of Biochemistry and Molecular Biology
246 Noble Research Center, Oklahoma State University
Stillwater, OK 74078 (USA)

Supporting information and the ORCID identification number(s) for the author(s) of this article can be found under <https://doi.org/10.1002/anie.202015422>.

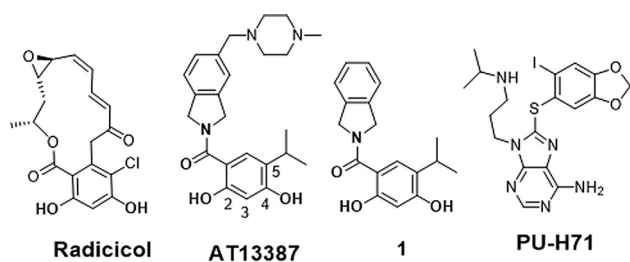


Figure 1. Structures of radicicol, AT13387, compound 1 and PU-H71.

(PDB:1UYM) revealed the presence of an extensive hydrogen-bond network that is coordinated by three conserved water molecules (labeled as A–C, Figure 2). However, the presence of Ser52 and Ile91 in Hsp90 α in lieu of Ala52 and Leu91 in Hsp90 β results in formation of a smaller hydrophilic pocket in Hsp90 α and a large hydrophobic subpocket in Hsp90 β . The subtle difference between these two binding sites were exploited to develop **KUNB31**, but unfortunately, the presence of a smaller pocket in Hsp90 α prevents such investigation. Thus, Ser52/Ala52 represents the only amino acid difference that can be utilized to develop Hsp90 α -selective inhibitors (Figure 2). Since compound **1** manifested equipotent binding affinity towards both Hsp90 α and Hsp90 β when evaluated in a fluorescence polarization (FP) assay (SI, Figure 3S), it served as a starting point for the development of Hsp90 α -selective inhibitors.

As can be seen in Figure 2, The resorcinol pharmacophore was shown to interact with Asp93 via the 2-phenol, whereas Ser52 hydrogen bonds with the 4-phenol via water molecules A and B. Therefore, systematic removal of each phenol was pursued to determine their contribution towards the binding to each isoform. Upon preparation, the desphenol variants, compound **2** (2-phenol) and compound **3** (4-phenol) (Figure 3) were evaluated for isoform selectivity.^[21,22] Compound **3**, which contains the 4-phenol, exhibited ≈ 10 -fold greater binding affinity for Hsp90 α versus Hsp90 β , whereas compound **2** bound Hsp90 β with minimal preference (≈ 2 -fold).^[21] Excited by these results, the isopropyl moiety at the 5-position was replaced to modulate the steric and electronic environment of the phenol, as well as to access the open

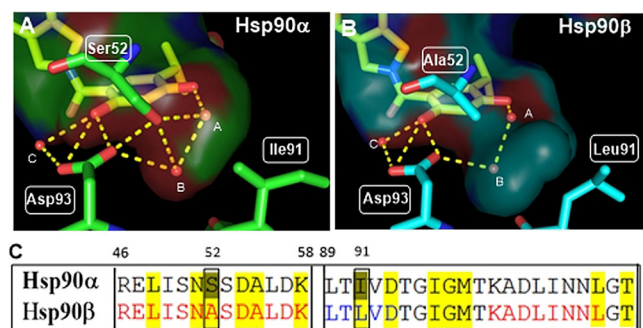


Figure 2. Resorcinol pharmacophore of compound 1 and its interactions with N-terminal ATP binding site in A) Hsp90 α and B) Hsp90 β C) Amino acid sequence alignment of N-terminal ATP-binding site (details in SI).

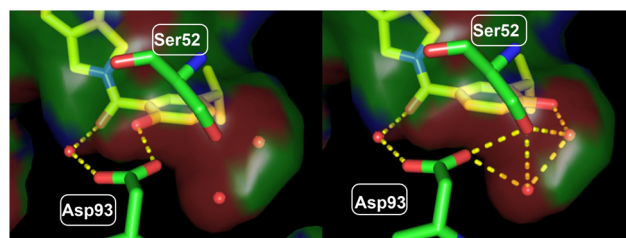
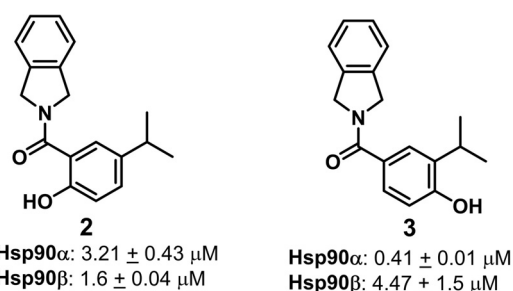


Figure 3. Screening of phenols **2** and **3** and their proposed binding modes in Hsp90 α (PDB code: 2XAB) and IC₅₀'s as determined with a fluorescence polarization (FP) assay. Compounds were incubated with Hsp90 α/β and FITC-GDA in triplicate, and IC₅₀ \pm SD was measured.

conformation of Hsp90 (Figure 4). Replacement of the 5-isopropyl substituent with a chlorine atom resulted in ≈ 10 -fold decrease in affinity, while the inclusion of iodine completely negated affinity. Introduction of bromine at the 5-position provided the highest selectivity (> 30 -fold) and a reasonable IC₅₀ of $\approx 2.73 \mu\text{M}$. Intramolecular hydrogen-bonding interactions between the fluorine and phenol hydrogen could explain the decreased affinity that was observed for compound **7**. Inclusion of a *t*-butyl group at the 5-position was shown to manifest affinity similar to **5**, and supports the hypothesis that spheric bulk elicits selectivity for Hsp90 α . Compounds **10**, **11** and **12** were synthesized to probe Site 1 of Hsp90 α (Figure 4, 4S), which is a flexible pocket that is lined with hydrophobic residues, while simultaneously reducing the distance between the 4-phenol and Ser52 to increase binding affinity and selectivity towards Hsp90 α .

The binding affinity of **10**, **11** and **12** were determined and compound **12** was found to bind Hsp90 α with a IC₅₀ of $\approx 4.8 \mu\text{M}$ and > 20 -fold selectivity versus Hsp90 β . As illustrated in Figure 4, the methylenedioxy ring induces the opening of Site 1, (Figure 4A, 4S). In contrast to **PU-H71**, which is a pan inhibitor that induces the opening of Site1, Compound **1** binds to the closed form of Hsp90 (Figure 4B).

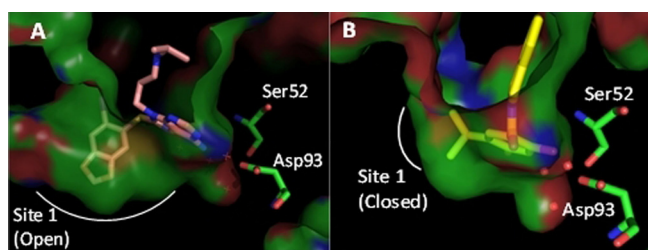
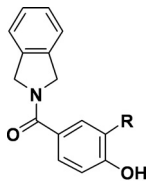


Figure 4. A) Co-crystal structures of **PU-H71** (PDB code: 2FWZ) and B) **1** (PDB code: 2XAB) with Hsp90 α .

Table 1: Replacement of the isopropyl group, IC_{50} determined using fluorescence polarization (FP) assay. Compounds were incubated with Hsp90 α/β and FITC-GDA in triplicate, and $IC_{50} \pm SD$ was measured.

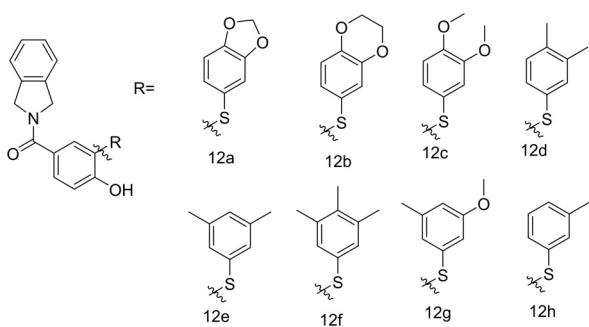


Compound	R group	IC_{50} Hsp90 α (μ M) ^(a)	IC_{50} Hsp90 β (μ M) ^(a)
4	Cl	4.69 \pm 0.27	> 100
5	Br	2.73 \pm 0.19	> 100
6	I	> 100	> 100
7	CF ₃	7.90 \pm 1.18	> 100
8		2.62 \pm 0.08	> 100
9		0.65 \pm 0.04	12.92 \pm 1.92
10		> 50	> 50
11		> 25	> 50
12		4.87 \pm 0.29	> 100

However, the 5-position thiophenol present in **12** is able to access Site 1 in a conformation that overlaps with the methylenedioxy ring of **PU-H71** (Figure 4SC). Despite the presence of an identical Site 1 in both Hsp90 α and Hsp90 β , substitutions on the thiophenol were proposed to elicit different conformations of Hsp90 α , perturbing interactions of the 4-Phenol with Ser52. Table 2 represents thiophenol analogs that were studied as well as their respective binding affinities (additional structure activity relationship (SAR), FP probe binding affinities for Hsp90 isoforms and solubility data can be found in supporting information). Compounds **12a** and **12b** contained methylenedioxy and ethylenedioxy rings, respectively, which were proposed to interact with Tyr139 via an additional hydrogen bond (Figure 5a).

As predicted by our model, compounds **12a** and **12b** were shown to exhibit improved binding affinity for Hsp90 α . Similarly, **12c**, which contained the 3,4-dimethoxy group bound Hsp90 α with an IC_{50} value of \approx 530 nM and \approx 22-fold selectivity versus Hsp90 β . A methyl scan on the thiophenol ring led us to conclude that substitutions at 3- and 4-positions enhanced binding affinity. Consequently, substitutions at the 3- and 4-position of the thiophenol ring were sought, and eventually resulted in the preparation of **12d**, **12e**, **12f**, and **12g**. Notably, **12d** and **12e** were found to exhibit an $IC_{50} \approx$ 840 nM and \approx 720 nM for Hsp90 α , whereas, the trimethyl substituted compound **12f** bound with reduced affinity. The 3-methoxy-5-methyl substituted compound (**12g**) resulted in \approx 900 nM affinity for Hsp90 α . Homologation of the 3-methyl substituent to the ethyl variant resulted in increased affinity. However, inclusion of a propyl group at the 3-position reduced affinity for Hsp90 α (SI).

Table 2: Installation of substituted thiophenols and evaluation of binding affinity IC_{50} determined using fluorescence polarization (FP) assay. Compounds were incubated with Hsp90 α/β and FITC-GDA in triplicates and $IC_{50} \pm SD$ was measured.



Compound	IC_{50} Hsp90 α (μ M) ^(a)	IC_{50} Hsp90 β (μ M) ^(a)	Fold Selectivity
12a	0.71 \pm 0.03	> 50	> 70
12b	0.52 \pm 0.01	27.7 \pm 3.07	\approx 53
12c	0.53 \pm 0.07	11.6 \pm 1.07	\approx 22
12d	0.84 \pm 0.13	> 50	\approx 63
12e	0.72 \pm 0.08	37.5 \pm 3.8	\approx 51
12f	3.03 \pm 0.26	> 50	> 16
12g	0.9 \pm 0.02	> 50	> 16
12h	0.46 \pm 0.05	22.28 \pm 2.8	\approx 48

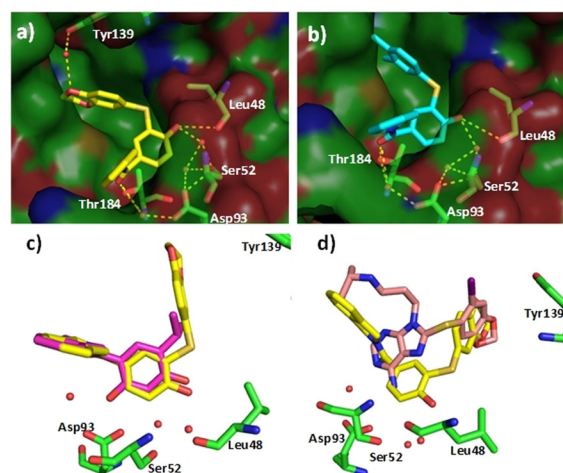


Figure 5. a) Co-crystal structure of **12b** with Hsp90 α (PDB code: 7LSZ) b) Co-crystal structure of **12d** with Hsp90 α (PDB code: 7LTO) c) Overlay of the co-crystal structures of **12b** and **1** bound to Hsp90 α (PDB: 2XAB) d) Overlay of the co-crystal structures of **12b** and **PU-H71** bound to Hsp90 α .

In order to study the binding mode of the Hsp90 α -selective inhibitors, compounds **12b** and **12d** were co-crystallized with the N-terminal domain of Hsp90 α . As expected, the crystal structures supported our hypothesis that the ethylenedioxy ring interacts with Tyr139 via a conserved water molecule, which increases binding affinity. In contrast, compound **12d** does not afford secondary hydrogen bond with Tyr139. However, the hydrophobic occupation of Site 1 improves the binding affinity by reducing the entropic penalty, which explains the increased affinity manifested by **12h**. It should also be noted that the 4-phenol interacts with

Ser52 via water molecules A and B (Figure 2 and Figure 5a,b). Therefore, the selectivity manifested by the benzenethiol containing compounds for Hsp90 α was rationalized by overlaying the binding pose of the non-selective compound **1**, and **12b** bound to Hsp90 α . As can be observed in Figure 5c, inclusion of the benzenethiol at the 5-position and the 4-phenol induce a conformational change that leads to the opening of Site 1. In fact, the orientation of the thioether fragment is different to that observed for the purine-class of Hsp90 pan-inhibitors (Figure 5d). The co-crystal structures of Hsp90 α bound to **12b** and **12d** suggest the thioether to shift toward the adenine binding pocket (Figure 5c) by bringing the 4-phenol into close proximity to Ser52, a residue that differentiates the Hsp90 α and Hsp90 β binding sites.^[16,17] As a result, Hsp90 α preferentially accommodates the benzenethiol containing 4-phenol.

A NCI-60 cancer cell screen was performed with compounds **5** and **12d** to determine the cellular response of Hsp90 α -selective inhibitors. The growth of non-small cell lung cancer cell line, NCI-H522, melanoma cell line UACC-62, ovarian cancer cell line SK-OV-3, and renal cell carcinoma cell line UO-31 were selectively inhibited. Hsp90 client protein degradation was determined using NCI-H522 cells treated with increasing concentrations of **12h**. In particular, the levels of Hsp90 client proteins Her2, Raf-1 and Akt decreased in a dose-dependent manner.

The Hsp90 β -dependent substrate, CDK4, degraded at a higher concentration of **12h** in comparison to c-Src, which is a Hsp90 α -dependent client, highlighting preferential inhibition of Hsp90 α in the cellular environment.^[21,23] Hsp90 α -dependent client survivin also decreased in a dose-dependent manner when treated with **12h**. Levels of Hsp70 were induced albeit to a lesser extent, which is in contrast to Hsp90 pan-inhibitors such as GDA. Hsp90 levels were induced at lower concentrations of **12h**, similar to GDA, however, it decreased with higher concentrations of **12h**. Interestingly, levels of HSF1 also decreased upon treatment with **12h** but only at high concentrations.

The design and development of isoform-selective inhibitors has remained a challenging task in medicinal chemistry, especially, when there exists significant sequence and conformational identity. Hsp90 α and Hsp90 β represent a major challenge for medicinal chemists, as only two amino acids vary in the ligand binding sites, and they are shielded behind two conserved water molecules. While an Hsp90 β -selective inhibitor was previously shown to occupy the small subpocket in Hsp90 β that results from the two amino acid difference, Hsp90 α -selective inhibitors could not be developed via a similar approach. Therefore, the roles played by each phenol was interrogated and led to the identification of monophenol **3** as a new lead compound that exhibited ≈ 10 -fold selectivity for Hsp90 α . Subsequent studies led to the development of compound **5**, which exhibited greater selectivity for Hsp90 α , but possessed modest binding affinity ($IC_{50} \approx 2.7 \mu M$.) Improvement in the binding affinity was sought by installation of a benzenethiol moiety to occupy Site 1. Further exploration of the benzenethiol side chain led to **12h**, which manifested an IC_{50} of ≈ 460 nM for Hsp90 α and ≈ 48 -fold selectivity over Hsp90 β . NCI Screening of the Hsp90 α -

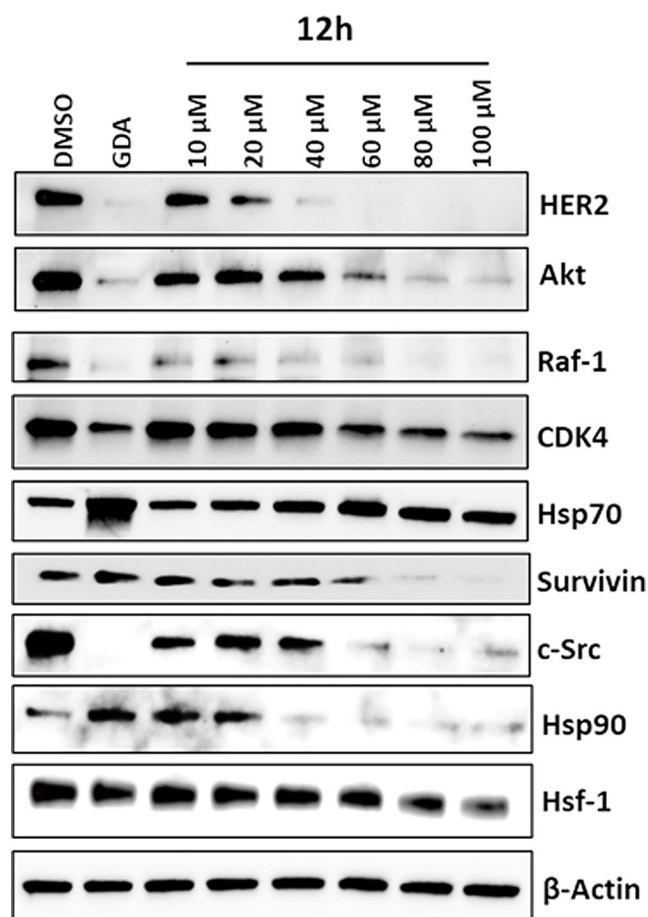


Figure 6. Western blot analysis of client proteins with **12h** in NCI-H522 cell line. DMSO and 500 nM Geldanamycin (GDA) were used as negative and positive controls, respectively.

selective inhibitors revealed cancer cell lines that are selectively inhibited by these compounds. Moreover, it was determined that Hsp90 α -dependent substrates are readily degraded in the presence of Hsp90 α -selective inhibitors, but Hsp90 β -dependent clients were not affected until higher concentrations were reached. In total, the first Hsp90 α -selective inhibitor was developed via a structure-based approach to yield a drug-like small molecule that manifests good affinity and reasonable selectivity in both recombinant and cellular assays. The full utility and optimization of these inhibitors continue and the results from such studies will be reported in due course.

Acknowledgements

The authors gratefully acknowledge financial support of this work via the National Institutes of Health to B.S.J.B. (CA213566), R.L.M. and J.D. (CA219907), and the Oklahoma Agricultural Experiment Station to R.L.M. (OKL03159) and J.D. (OKL03060). The research is also supported in part by an Institutional Development Award (IDeA) from the National Institute of General Medical Sciences of the National Institutes of Health (Award

P20GM103640). We thank the staff of beam-line 14 at the Stanford Synchrotron Radiation Lightsource for their support.

Conflict of interest

The authors declare no conflict of interest.

Keywords: drug discovery · Hsp90 alpha · isoform selectivity · structure-based drug design

-
- [1] M. Taipale, D. F. Jarosz, S. Lindquist, *Nat. Rev. Mol. Cell Biol.* **2010**, *11*, 515–528.
- [2] H.-K. Park, N. G. Yoon, J.-E. Lee, S. Hu, S. Yoon, S. Y. Kim, J.-H. Hong, D. Nam, Y. C. Chae, J. B. Park, B. H. Kang, *Exp. Mol. Med.* **2020**, *52*, 79–91.
- [3] M. V. Powers, P. Workman, *FEBS Lett.* **2007**, *581*, 3758–3769.
- [4] L. Neckers, P. Workman, *Clin. Cancer Res.* **2012**, *18*, 64–76.
- [5] V. C. da Silva, C. H. Ramos, *J. Proteomics* **2012**, *75*, 2790–2802.
- [6] J. M. Holzbeierlein, A. Windsperger, G. Vielhauer, *Curr. Oncol. Rep.* **2010**, *12*, 95–101.
- [7] K. Jhaveri, T. Taldone, S. Modi, G. Chiosis, *Biochim. Biophys. Acta Mol. Cell Res.* **2012**, 1823.
- [8] A. Yuno, M. J. Lee, S. Lee, Y. Tomita, D. Rekhman, B. Moore, J. B. Trepel, *Methods Mol. Biol.* **2018**, *1709*, 423–441.
- [9] D. S. Hong, U. Banerji, B. Tavana, G. C. George, J. Aaron, R. Kurzrock, *Cancer Treat. Rev.* **2013**, *39*, 375–387.
- [10] A. Hoter, M. E. El-Sabban, H. Y. Naim, *Int. J. Mol. Sci.* **2018**, *19*, 2560.
- [11] X. Wang, X. Song, W. Zhuo, Y. Fu, H. Shi, Y. Liang, M. Tong, G. Chang, Y. Luo, *Proc. Natl. Acad. Sci. USA* **2009**, *106*, 21288–21293.
- [12] W. Li, D. Sahu, F. Tsen, *Biochim. Biophys. Acta Mol. Cell Res.* **2012**, *1823*, 730–741.
- [13] B. K. Eustace, T. Sakurai, J. K. Stewart, D. Yimlamai, C. Unger, C. Zehetmeier, B. Lain, C. Torella, S. W. Henning, G. Beste, B. T. Scroggins, L. Neckers, L. L. Ilag, D. G. Jay, *Nat. Cell Biol.* **2004**, *6*, 507–514.
- [14] J. E. Bohonowych, M. W. Hance, K. D. Nolan, M. Defee, C. H. Parsons, J. S. Isaacs, *Prostate* **2014**, *74*, 395–407.
- [15] A. K. Voss, T. Thomas, P. Gruss, *Development* **2000**, *127*, 1–11.
- [16] I. Grad, C. R. Cederroth, J. Walicki, C. Grey, S. Barluenga, N. Winssinger, B. De Massy, S. Nef, D. Picard, *PLoS One* **2010**, *5*, e15770.
- [17] C. Kajiwara, S. Kondo, S. Uda, L. Dai, T. Ichianagi, T. Chiba, S. Ishido, T. Koji, H. Udono, *Biol. Open* **2012**, *1*, 977–982.
- [18] A. S. Duerfeldt, L. B. Peterson, J. C. Maynard, C. L. Ng, D. Eletto, O. Ostrovsky, H. E. Shinogle, D. S. Moore, Y. Argon, C. V. Nicchitta, B. S. J. Blagg, *J. Am. Chem. Soc.* **2012**, *134*, 9796–9804.
- [19] P. D. Patel, P. Yan, P. M. Seidler, H. J. Patel, W. Sun, C. Yang, N. S. Que, T. Taldone, P. Finotti, R. A. Stephani, D. T. Gewirth, G. Chiosis, *Nat. Chem. Biol.* **2013**, *9*, 677–684.
- [20] S. J. Mishra, S. Ghosh, A. R. Stothert, C. A. Dickey, B. S. Blagg, *ACS Chem. Biol.* **2017**, *12*, 244–253.
- [21] A. Khandelwal, C. N. Kent, M. Balch, S. Peng, S. J. Mishra, J. Deng, V. W. Day, W. Liu, C. Subramanian, M. Cohen, J. M. Holzbeierlein, R. Matts, B. S. J. Blagg, *Nat. Commun.* **2018**, *9*, 425.
- [22] C. W. Murray, M. G. Carr, O. Callaghan, G. Chessari, M. Congreve, S. Cowan, J. E. Coyle, R. Downham, E. Figueroa, M. Frederickson, B. Graham, R. McMenamin, M. A. O'Brien, S. Patel, T. R. Phillips, G. Williams, A. J. Woodhead, A. J. A. Woolford, *J. Med. Chem.* **2010**, *53*, 5942–5955.
- [23] W. Liu, G. A. Vielhauer, J. M. Holzbeierlein, H. Zhao, S. Ghosh, D. Brown, E. Lee, B. S. Blagg, *Mol. Pharmacol.* **2015**, *88*, 121.

Manuscript received: November 20, 2020

Accepted manuscript online: February 23, 2021

Version of record online: March 26, 2021